地形 第12巻第1号
1-24頁 (1991)

JGU Transactions, Japanese Geomorphological Union
12-1 p. 1-24 (1991)

Stochastic Aspects of the Relations between Climate, Hydrology and Landform Evolution*

Thomas DUNNE**

Abstract

The frequency distributions of rainstorm characteristics control the timing, magnitude, and spatial pattern of runoff and resulting sediment redistribution. Therefore, they influence the nature of landform evolution. Two examples are presented of how the frequency distributions of rainstorm intensity and duration characterizing a climate affect hydrologically driven landform evolution. In the first case it is shown that sheetwash erosion, which is usually thought to produce concave hillslope profiles in the presence of a stable base level, can generate convex profiles under climates with sufficiently skewed frequency distributions of rainfall intensity and duration. The second case describes relationships between these same climatic parameters and the spatial and temporal distribution of landsliding within bedrock hollows in humid mountain landscapes. The stochastic nature of landslide occurrence in a hollow affects not only the size of the scar and position of its headscarp for hundreds of years, but also the timing and magnitude of debris-flow scour and deposition in low-order valleys downstream of the hollow.

Key Words: *Climatic geomorphology, Hydrogeomorphology, Hillslope evolution, Sheetwash, Mass wasting.*

Climate and Landforms

The nature and relative importance of climatic influences on landform evolution have been debated since the earliest days of theoretical geomorphology, as indicated in the classic papers collected by Derbyshire (1973). Most of the pertinent literature discussed one or other of the following issues: (1) whether it is possible to recognize distinctive assemblages of landforms that characterize climatic and biogeographical regions; 2 whether assemblages of landforms reflect interactions of suites of geomorphic processes, the distributions of which do not necessarily coincide with climatic regions defined in terms of mean climatological parameters. Until the 1970s, the traditional methods of studying the relationships between climate and landforms involved either: regional classification of landforms that were assumed to bear simple relationships to the regionally-averaged climate, biota, and soils, or deductive reasoning

Received July 2, 1990: accepted August 8, 1990.

* This paper is based upon an address presented at the 10th Anniversary Meeting of the Japanese Geomorphological Union in Kyoto in 1989.

** Department of Geological Sciences, University of Washington, Seattle, WA 98195, USA.

about how an observed or hypothesized set of processes, with varying assumed relative efficacies, might produce characteristic landforms. During that decade, it became apparent that geomorphologists needed to concentrate more research effort on how the climatically driven processes generate landforms.

In a compilation edited by Derbyshire (1976), authors reviewed the information from theory and field studies concerning climatic effects on geomorphic processes in many regions. However, there was little success at formally relating climatically driven processes to landform evolution. Only the chapter by Kirkby (1976) contained formal mathematical models of some aspects of this relationship. Specifically, he modelled how climate affects hillslope hydrology, including runoff, soil-moisture storage, and evapotranspiration. He then hypothesized relationships between evapotranspiration and vegetation cover density and between the latter and soil-moisture storage capacity. Annual rainfall, which drives the model, is assumed to be distributed into a frequency distribution of daily rainfalls:

$$N(r) = Ne^{-r/r_0} \tag{1}$$

where $N(r)$ is the annual number of raindays with rainfall in excess of r, N is the total number of raindays per year, and r_0 is the mean rainfall per rainday ($=R/N$), and R is the total annual rainfall. Because of the use of 24-hour average rainfall intensities, the model is only applicable to environmental conditions which do not generate Horton overland flow. The predicted annual totals of saturation overland flow and subsurface flow are related to annual rates of soil wash and solute transport on the basis of approximate theoretical and field-based expressions. The rates of sediment and solute transport are then inserted into a mass-balance analysis of regolith for computation of the simulaneous evolution of hillslope profiles and soil depths.

Approach of the Current Study

This paper briefly describes two ongoing investigations of the effects of climate on landforms. Both are rooted in the spirit of Kirkby's process-based approach relating climate and landform evolution through hydrology. They are also examples of what Okunishi (1981) defined as hydrogeomorphology: "a division of study that makes clear the interaction between the hydrologic cycle and changing processes of landforms."

Computations of landform shape based on models of the linkages between runoff and erosion processes require the input of climatic parameters, whether explicitly or implicitly. For example, Horton's (1945) pioneering effort to predict the extent of hillslope concavities (beyond his critical distance for sheetwash erosion) requires the

insertion of a rainfall intensity, and implicitly, a storm duration and frequency. Roth et al. (1989, Fig. 4) provide an example of an analytical solution for a Horton hillslope profile. Once the initial gradient, particle size, hydraulic roughness, critical shear stress, and infiltration capacity have been set, a single value of rainfall intensity must be chosen to represent the climate in the solution of the characteristic hillslope profile. The threshold-slope mass-wasting model of Carson and Petley (1970) incorporates the assumption that rainstorms large enough to saturate soil profiles to the surface occur frequently enough for mass failure to control the characteristic angles of straight hillslope segments in a region. Thus, a minimum rainstorm intensity and duration, and therefore frequency, are implied. Okunishi and Iida (1981) made a similar assumption in their analysis of the critical thickness to which colluvium develops before landsliding occurs.

The selection of a rainstorm of a particular intensity, duration and frequency for modeling the relationship between climate and landforms allows the solution of an equation predicting a static, stable landform geometry. By contrast, Kirkby's (1976) model takes into account the full frequency distribution of rainstorm intensity (for a single duration), and it allows the interaction of runoff generated by this frequency distribution with the evolving soil depth and hillslope shape. The examples of climate-hydrology-landform models described here illustrate in more detail the importance of (a) taking account of the frequency distribution of rainstorm intensities and duration, and (b) the interaction of rainstorm occurrence and the evolving characteristics of colluvium. However, for the sake of simplicity, the examples do not incorporate the effect of climate on weathering. An unlimited supply of colluvium is assumed to be available for erosion.

Figure 1 indicates the approach of this study to the interrelationships between climate, hydrology, and the erosion of landforms. Since the concern is with specific processes which occur on the time scale of single rainstorms, it is necessary to examine the climate on that time scale. Thus, the climate is regarded as stochastic, and is characterized by frequency distributions of rainstorm intensity, duration and temporal spacing. The moments of these distributions vary between climatic regions (e.g., Beven, 1986), but climatic statistics are not widely available in a form that is useful for hydrological and geomorphological modeling. Another climatic factor of geomorphological importance is that climate changes over the life span of most landforms, and therefore changes the moments of these distributions. Since paleoclimatologists can reconstruct only average measures of climate, it may be necessary to estimate intensity-duration-frequency regimes of past climates by correlating current rainfall statistics with climatic mean values and then substituting space for time.

Once the climate is characterized by the rainstorm frequency distributions (from

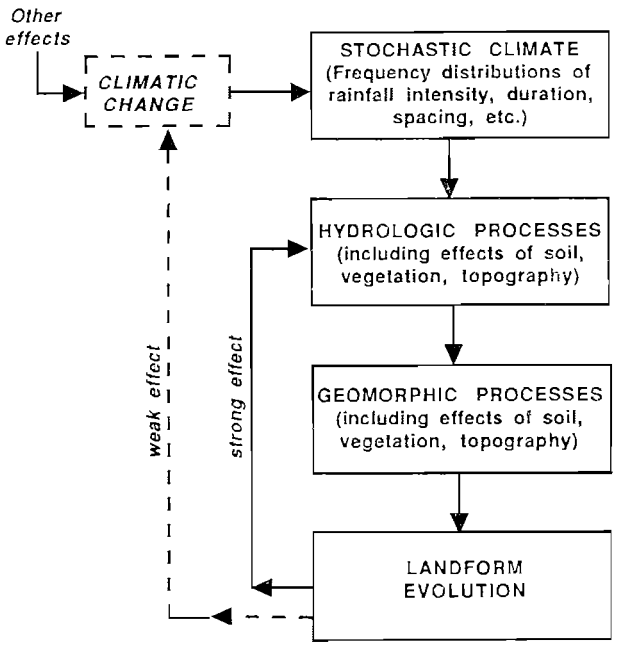

Fig. 1. Relationships between climatic characteristics, hydrologic processes, geomorphic processes and landform evolution.

instrumental records, analysis of regional relationships, or paleoclimatology, related biotic characteristics, such as vegetation type, and density may also be defined. Sequences of rainstorms can then selected at random from the frequency distribution to drive deterministic models of runoff. The particular dominant runoff process is also largely determined by the regional climate and vegetation since these are the first-order effects on the rainfall intensity and infiltration capacity which determine whether runoff occurs over or beneath the ground surface (Figure 2), although soil characteristics, and topography also play an important role at the local scale.

In this paper, examples of the role of Horton overland flow on African savanna hillslopes and of subsurface stormflow typical of the humid forested Pacific Rim are described. The event-based models of runoff processes in these environments incorporate the effects of rainstorm intensity and duration (interstorm spacing is ignored at present), soil characteristics, vegetation, and topography. Random spatial effects due to heterogeneities of soil properties may be significant, but have not been studied in a manner that allows any general principles to be defined, and these effects are ignored here.

Runoff processes drive the erosion and sediment transport which redistribute soil and alter landform shape. In the African example, Horton overland flow is responsible

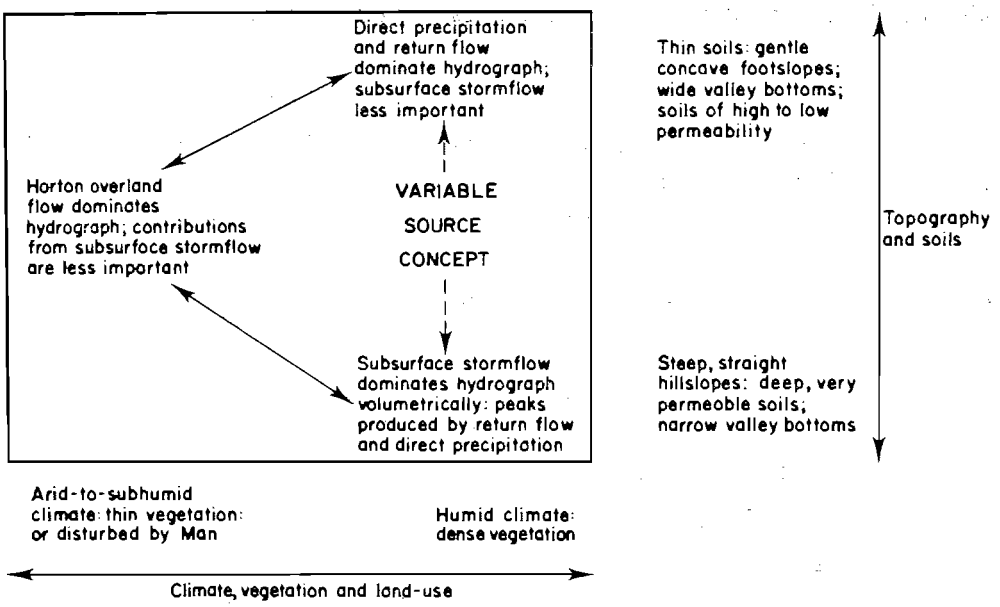

Fig. 2. Dominant factors controlling the processes generating storm runoff (Dunne, 1978).

for sheetwash; in the Pacific Rim example, pore-pressure fields developed in subsurface flow trigger landslides and debris flows, and the resulting scar is filled by soil creep. Deterministic models of these processes, incorporating the effects of soil properties and vegetation, redistribute regolith and alter landform characteristics. In the African case, this approach is applied to the evolution of hillslope profiles; in the Pacific Rim example the concern is with the evolution of colluvial wedges (Dietrich and Dunne, 1978, p. 197) which accumulate in zero-order basins and are the sources of landslides and debris flows (Tsukamoto et al., 1982, Benda and Dunne, 1987; Shimokawa et al., 1989). The models described here predict the evolution of landform characteristics.

Evolution of landform shape or other property causes strong feedbacks on the hydrologic processes that are driving the erosion because the initial and boundary conditions for each runoff event are different from those of its predecessor. These effects are taken into account in the models discussed below which simulate 10^4–10^5 years of erosion. There may also be weaker feedbacks of landform evolution on climate, either because the lowering of elevation reduces precipitation, or because the changing shape of the landform causes rainfall to be distributed differently onto the soil surface. However, the main factors affecting climatic change, and therefore the important rainfall frequency distributions driving the hydrogeomorphic models

discussed here, are external to the landscapes being considered.

Convex Profiles on Savanna Hillslopes

Over large areas of the craton of eastern Kenya typical hillslopes are long (500-1000 m) with low overall gradients (0.01-0.1) and long convex upper profiles (50-500 m). A graph of gradient versus downslope distance for a typical hillslope is shown in Figure 3. The proportion of the profile that is convex varies from 5 to 80 percent as the overall gradient of the entire hillslope decreases from 0.08 to 0.01.

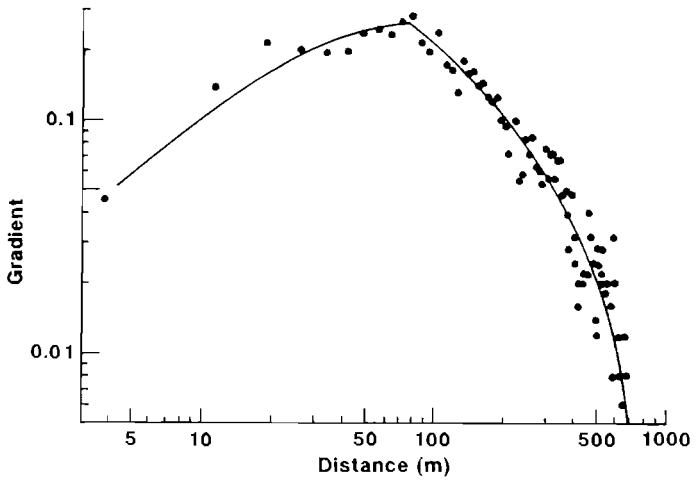

Fig. 3. Graph of gradient versus distance for a typical hillslope profile in eastern Kenya. Each point represents a segment surveyed with a tape and hand level.

The landscape is developed mainly in Precambrian schists and gneisses which weather to reddish sandy clay loams, generally less than 1.0 m deep. Mean annual precipitation in the region ranges from 250 to 750 mm, concentrated in two seasons centered on March-April and November-December with strong intervening dry seasons. The natural vegetation is woodland, bushland and grassland, but widespread burning and grazing have caused a reduction in woody plants and much of the landscape now has only a thin ground cover. Under both disturbed and natural cover (the latter being observable in national parks) there is widespread field evidence of Horton overland flow and sheetwash erosion, although rills and gullies are of only local extent, expect around roads and settlements.

Current theories of hillslope evolution without rapid base-level lowering associate the convex part of the profile with erosion by diffusive sediment transport processes (Hirano, 1968; Kirkby, 1971; Ahnert, 1976; Smith and Bretherton, 1972). Under the

climatic and vegetation conditions which produce Horton overland flow, rainsplash is usually identified as this diffusive process (DePloey and Savat, 1968; Kirkby, 1971; Ahnert, 1976; Mosley, 1973; Band, 1985), whereas sheetwash is thought to generate the concave profile further downslope (Kirkby 1971; Ahnert, 1976; Band, 1985).

Each of the authors referred to above has analyzed hillslope profiles by means of the continuity equation for sediment transport into which they inserted an equation for the sediment flux:

$$\frac{\partial z}{\partial t} = -\frac{1}{\rho_b}\frac{\partial q_s}{\partial x} \tag{2}$$

$$q_s = \mathrm{F}(s, q), \tag{3}$$

where x, z and t are spatial and temporal coordinates, ρ_b is the soil bulk density, s is the local gradient, and q and q_s are respectively the fluxes of water and sediment per unit width of hillslope. The value of q_s required for Equations (2) and (3) refers to the long-term average sediment transport, whereas most studies relating soil erosion processes to their controlling factors measure the instantaneous or annual rates of sediment transport. Since these short-term rates fluctuate strongly with rainfall input, they must be integrated over the frequency distributions of rainfall intensity and duration that characterize the climate to produce a long-term sediment transport equation.

Kirkby (1971, 1976, 1986) and Carson and Kirkby (1972, p. 204, p. 216), Mosley (1973) and Band (1985) used the results of various small-plot studies of erosion conducted over one or more experiments or seasons to obtain exponents for long-term sediment transport equations of the form proposed by Hirano (1968):

$$q_s = kq^m s^n. \tag{4}$$

The results suggest that the values of m and n for sheetwash lie in the range of 1.0–2.0, while for rainsplash, $m=0$ by definition, and $n \leq 1$. These authors have shown that for constant-form hillslopes, and for hillslope eroding with a fixed base level, values of $m<1$, $n>0$ in Equation (4) are required for the development of convex profiles. Such conditions are usually associated with rainsplash and soil creep.

These results suggest that the convex upper profiles of the Kenyan hillslopes described above have been formed by rainsplash. However, on the convexities there is evidence of intense sheetwash, even in national parks grazed only by wildlife. Bare areas of the soil surface exhibit wash marks, and during artificial rainstorms on 5 m- and 6 m-long plots I have measured rates of sheetwash transport far larger than those of rainsplash. It is thus hypothesized that on the hillslopes studied in eastern Kenya, convexities on the scale of 100 m or more are formed mainly by sheetwash,

although rainsplash obviously contributes to the rounding of the profile.

The data used to test this hypothesis were collected during experiments under artificial rainstorms on plots 5 m long and 1.2 to 2.0 m wide on hillslopes in Kajiado District, southeastern Kenya. The rainfall simulator used was described by Dunne et al. (1980). The nature of the sheetflow and its cross-slope and alongslope variability were described by Dunne and Dietrich (1980). During the experiments, rainfall intensities and instantaneous runoff rates were measured and used to calculate infiltration rates, which reached constant rates after 10–30 minutes in most experiments. Average flow depths and velocities were measured at one-meter intervals along the plots at steady-state runoff, and were used to calculate apparent Darcy-Weisbach friction factors for the flow through the microtopography and vegetation cover of the experimental surfaces. The friction factors and associated Reynolds Numbers were used to generate Moody diagrams for various vegetation cover densities. The hydraulic roughness reflected by this relationship is dominated by ground cover density, but also reflects the influence of microtopography.

The data on hydraulic roughness and the steady-state infiltration capacities collected in this way were used in a numerical model of one-dimensional flow employing the kinematic-wave approximation and solving by means of the Lax-Wendroff finite-difference scheme. The model produced values of discharge, flow depth, and total boundary shear stress throughout a rainstorm of any duration and constant intensity for any location on a hillslope with specified profile shape, infiltration capacity, and cover density. The computer program used for this purpose was developed by Reid (1989).

Instantaneous sheetwash transport rates from the plots were also measured during the field experiments, and correlated with the total shear stress in the flow calculated for the downslope end of the plot. A multiple regression analysis of these data yielded an equation for instantaneous sediment transport:

$$q_s = 4.85 \times 10^{-4} \tau^{1.32} C^{-0.76} \tag{5}$$

where q_s is the sediment flux per unit width (g/cm/sec), τ is the total boundary shear stress in the flow (dy/cm^2), and C is the ground cover density (%). The shear stress was obtained from

$$\tau = \rho g h s \tag{6}$$

where ρ is the density of water, g is the gravitational acceleration, h is the cross-slope averaged flow depth, and s is the plot gradient. The value of h at 5 m was calculated (to avoid the complication introduced by the drawdown of the water surface at the lip of the measuring trough) from the measured runoff rate and the friction-

factor/Reynolds Number relationship developed for the plot. Thus, the shear stress is used as a gross measure of transport capacity that integrates the effects of spatial variability in flow depth, velocity, and microtopographic slope, and includes the shear stress components that are not effective in transporting sediment.

Some of the measurements used to define Equation (5) were obtained from clay and sandy clay soils developed on Cenozoic volcanic rocks, as well as those obtained from the sandy clay loam on the Precambrian crystalline rocks. The three soils were compared in greater detail by Dunne and Dietrich (1980). There are almost certainly some differences in erodibility between these soils, but this effect seems to be of secondary importance. The values of sheetwash transport for intermediate cover densities 35-45% overlap for the clay and the sandy clay loam, possibly because much of the transport from the clay consisted of sand-sized aggregates which, like the sandy surface layer of the other two soils, travelled as a bedload layer through which finer particles diffused upward as a result of raindrop impacts. When larger differences in sheetwash transport due to soil erodibility are eventually isolated, however, relationships of the general form of Equation (5) will probably still pertain. With data currently available, it is not possible to separate the roles of shear stress and raindrop impacts in mobilizing sediment into sheetwash transport, since rainfall intensity affects the flow rate, depth, and therefore shear stress. Despite this uncertainty in physical understanding, Equation (5) provides a useful summary of the field measurements for the present purpose.

Values of flow depth from the runoff model and local values of hillslope gradient were used to calculate local values of τ, which were then used in Equation (5) to obtain sheetwash transport at any location on a hillslope at any time during a rainstorm. Values of total transport for each location during a storm were obtained and the downslope divergence of these values was used to obtain the local lowering rate, as indicated in Equation (2). Thus, a numerical form of Equation (2) was used to calculate the spatial pattern of hillslope lowering that results from each rainstorm. Figure 4 presents examples for an initially straight slope with a gradient of 0.05 and a fixed base level as a result of rainstorms of 4 different durations. These results indicate that in short storms, there is sediment transport everywhere on the straight hillslope, but only at the upper end is there a divergence of transport required for lowering. Thus, a short storm tends to produce an upper convexity. Longer storms, approaching the time of concentration for runoff from the slope, lower the surface on the footslope more than the upper part of the slope, tending to generate concavities. Over many storms, these spatial patterns change as they alter the hillslope profile.

The long-term pattern of erosion depends on the relative numbers of storms with

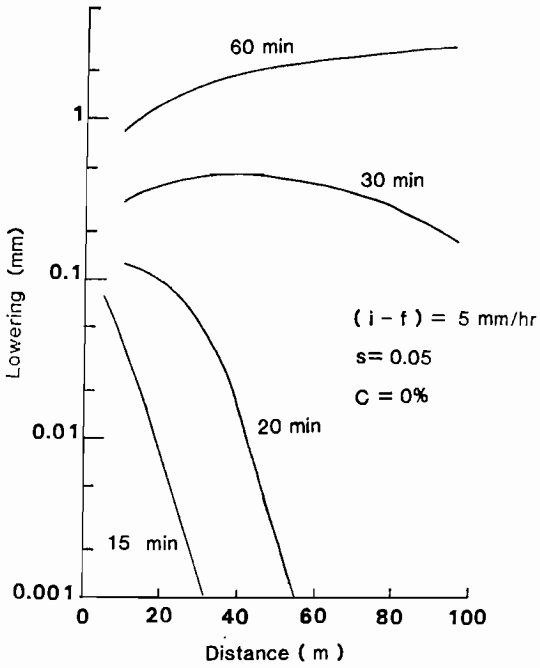

Fig. 4. Calculated amounts of lowering by sheetwash during rainstorms of 4 indicated durations which generated 5 mm/hr of runoff (rainfall intensity—infiltration rate) on a straight, bare hillslope with a gradient of 0.05.

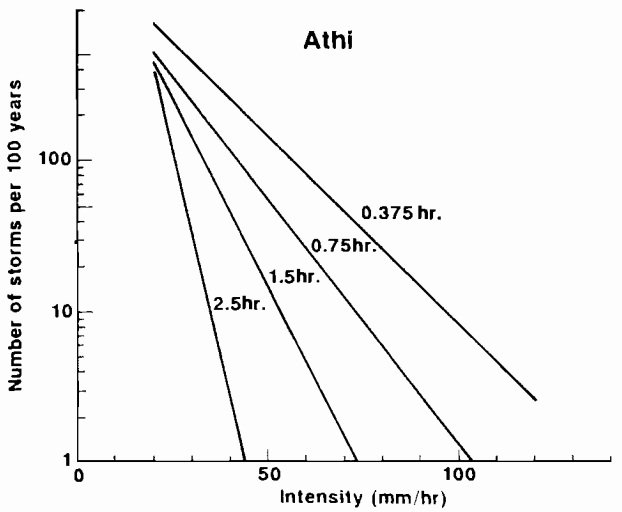

Fig. 5. Frequency of rainstorms of various durations and intensities for a station near Nairobi, Kenya.

different intensities and durations. Intensity-duration-frequency curves for a station near Nairobi, on the humid margin of the study area, were developed from an automatic rain-gauge record (Figure 5). Only 10 years of such data were available at the time of the study, but they are adequate for illustrating the principle of interest here. The runoff and erosion models were then run for all the storms expected in a 100-year period, and the resulting erosion pattern was used to change the initially straight hillslope shape. The new topography was then entered into the model, and the computation repeated in 100-year increments for 20,000 years. Figure 6 shows the result of 20,000 years of evolution under the intensity-duration-frequency regime characteristic of a climate with a mean annual rainfall of 750 mm. The average annual ground cover density in such an area would be approximately 75%.

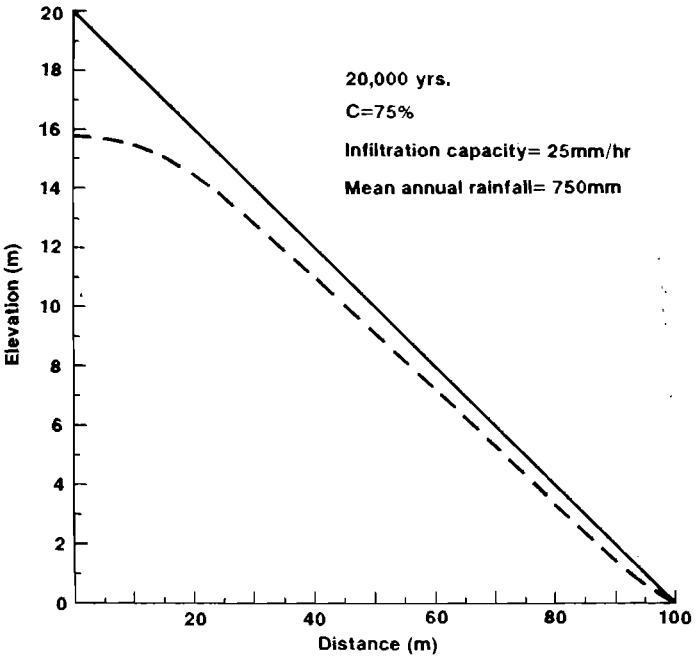

Fig. 6. Computed erosion of an initially straight hillslope into a convex profile as a result of 20,000 yrs of runoff and erosion under a vegetation cover density of 75% and the intensity-duration-frequency regime of a station with a rainfall of 750 mm/yr.

Because there is no flow and therefore no shear stress at the upper end of the profile ($x=0$), the computation results in a short spike of residual topography in the first increment of distance near the divide. This could be removed by adding to Equation (5) a term for rainsplash, which would by itself have produced a convex

profile. However, the purpose of the present calculation is to emphasize that sheetwash alone can generate convex hillslopes under certain climatic conditions. Therefore, the distance increments were limited to 10 m or less in all runs of the model. A separate calculation, based on field measurements of rainsplash transport on the experimental plots, indicates that a topographic spike of this width would be removed by rainsplash as quickly as the convexity downslope of it would be lowered by sheetwash.

The results indicate that under certain climatic regimes, characterized by a preponderance of rainstorms that are short relative to the time of concentration of runoff from the hillslopes, sheetwash generates convex slope profiles. The time of concentration, in turn, is affected by several climatically influenced factors, such as infiltration capacity and hydraulic roughness (which depend in part on ground cover density) and rainfall intensity, as well as by topographic and soil factors (Dunne and Dietrich, 1980). Runs of the computer model indicate that if all other factors are held constant, the lengths of the convex portions of hillslope profiles increase as rainstorm intensities and duration decrease, as infiltration capacity and ground cover density increase, as overall gradient decreases and as hillslope length increases. These results are in qualitative agreement with common field experience.

Accumulation and Failure of Colluvium in Bedrock Hollows

Dietrich and Dunne (1978) described a self-driven cycle of accumulation and failure of colluvium in bedrock hollows in the Coast Ranges of the Northwestern United States (Figure 7). Depths of colluvium in bedrock hollows are compared with those on nearby planar hillsides in Figure 8. Soil creep funnels colluvium into the convergent topography of bedrock hollows, where it accumulates for thousands of years. The centers of these same hollows also receive concentrated fluxes of subsurface flow, and therefore experience greater pore pressures than their surroundings. While the colluvium is thin, it is firmly anchored vertically and laterally by the roots of bushes and later of trees. As the colluvium thickens the density of roots anchoring it to bedrock diminishes and eventually the factor of safety decreases and failure occurs in the axis of the hollow. Tsukamoto et al. (1982) described the history of their own work on the same process, and introduced the term "zero-order" basin for what we called a bedrock hollow.

More recent work on these features has focused on: (1) the conditions under which the colluvium is stabilized and later destabilized after a critical depth is reached (e.g., Okunishi and Iida, 1981; Burroughs, 1984; Tsukamoto and Kusakabe, 1984; Tsukamoto and Minematsu, 1986; Reneau and Dietrich, 1987); (2) hydrologic conditions

Fig. 7. Colluvial wedge partly filling a U-shaped bedrock hollow in the Olympic Mountains, western Washington. Note the great depth of light-colored colluvium compared to the thinner soil on adjacent hillslopes. (Photo by L.M. Reid)

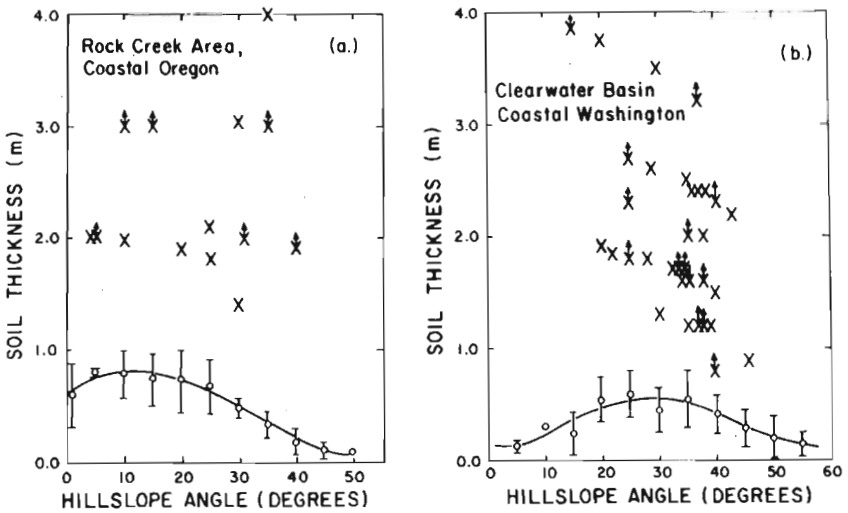

Fig. 8. Relationship of soil depth to hillslope angle on planar hillslopes (circles) and in bedrock hollows (crosses) for two mountain areas in the Pacific Northwestern USA. (Source: Dietrich et al., 1982).

associated with the failures (e.g., Wilson and Dietrich, 1987); and (3) the role of climatic change in driving episodes of filling and evacuation of the hollows (e.g., Reneau et al., 1986). In this paper, I will use highly simplified descriptions of these

factors to illustrate how the filling and failure of colluvial wedges in bedrock hollows results from the interplay of stochastic rainfall intensities and duration, and trends in the hydrologic and geotechnical properties of accumulating colluvium.

A bedrock hollow or zero-order basin usually consists of a strongly convergent portion, which can be approximated by a cone, employed by Iida (1984), and a slowly convergent, more linear section, for which Dietrich et al. (1986) introduced the term "tipped triangular trough". The relative sizes of these two sections varies from region to region with lithology and perhaps age of the feature. For the sake of simplicity of expression and computation, the calculations described below will be confined to the conical part of the features, which suffices to illustrate the interaction principle stated in the last sentence of the preceding paragraph.

The computation of accumulation and failure of the hollows consists of the following steps:

(1) Soil creep, bioturbation, and weathering supply colluvium to the conical hollow at a fixed rate. This supply is not modeled at present; it is simply assumed to be generated *in situ*, or to enter the bedrock hollow from cliffs or from a large reservoir of colluvium covering the adjacent hillside. The colluvium supply is spread uniformly over the conical surface, so that the soil depth increases each year. The supply rate presumably depends partly on climate as well as lithology and topography, but the few available field measurements (e.g., Dunne and Dietrich, 1978; Shimokawa, 1984; Shimokawa et al., 1989; Reneau et al., 1986) have not yet yielded any general principles.

(2) As the soil deepens, several of its geotechnical properties change. The critical concern for slope stability is the shear strength in the weakest part of the profile. Using "infinite-slope" assumptions, the slope stability equation for any level, y, below the colluvium surface can be crudely summarized as:

$$\gamma_s y \sin\theta \cos\theta = [c_s + c_r] + [\gamma_s - m\gamma_w] y \cos^2\theta \tan\phi \tag{7}$$

where γ_s and γ_w are the bulk densities of soil and water respectively, θ is the angle of the slope at failure, ϕ is the angle of internal friction of the colluvium, c_s is the cohesion between soil particles, c_r is the "apparent cohesion" due to plant roots, and m is the relative thickness of soil saturation ($=h/y$, where h is the thickness of the saturated layer above the level y). The value of y ranges from zero at the surface to a maximum, z, at the base of the colluvium. More complicated expressions for slope stability in forested bedrock hollows have been developed (e.g., by Humphrey, 1983, and Burroughs, 1984), but Equation (7) is adequate for illustrating the principles of interest here.

On the basis of a review of literature and field observations, it is suggested that

changes in several of the variables in Equation (7) may result from thickening of the colluvial wedge, and therefore from progressive burial and weathering. Some of the temporal changes are likely to be insignificant in climatic and tectonic regions where the average residence time of the colluvium is short, but they are all included here to stimulate discussion and field study.

Cohesion between soil particles is usually low in recently disturbed colluvium, but if the material remains below the root zone on a hillslope for time periods of the order of 10^4 years, the possibility exists for weathering reactions such as clay-mineral and oxide formation to increase the cohesion with time, and therefore with depth of burial. In the following calculation this effect is represented by a function

$$c_s = \alpha e^{\beta y} \tag{8}$$

where α and β could vary with lithology and climate, and could be studied on datable colluvial deposits. In the absence of such field data, values of $\alpha=1$, and $\beta=0.2$ as used here for illustration with SI units.

The effect of plant roots in providing an apparent cohesion depends on the density and strength of roots at any level. Since the density of roots decreases strongly below some depth for most plants, the potential for vertical roots to anchor colluvium to the bedrock must diminish strongly as the colluvium thickens. Although it is possible that there is a maximum anchoring effect at some intermediate colluvium depth due to plant succession, a monotonic function is used here to represent the resistance contribution of vertical root reinforcement. To represent the vertical anchoring by roots, I have chosen a function of the form

$$c_{vr} = \delta - e^{-\eta y} \tag{9}$$

with $\delta=16$ kPa and $\eta=2.0$, for $y<1.4$ m. Lateral roots anchor colluvium within the root zone and also resist strain softening below it, so to represent these effects I have used a hypothetical function

$$c_{lr} = \kappa - \lambda y \tag{10}$$

with $\kappa=10$ kPa and $\lambda=2.0$. Since the parameters of Equations (9) and (10) reflect biotic characteristics, they should also vary with climate.

Colluvium bulk density often increases with depth. Densification and, in old colluvium, weathering may also slowly increase the angle of internal friction. I have represented these associated effects by

$$\gamma_s = 10{,}000 + 2000 y^{0.5} \tag{11}$$

and

$$\tan\phi = 0.75 + 0.03\, y. \tag{12}$$

The cumulative effects of these various strength components at various depths in a colluvium profile are shown in Fig. 9. Curve 1 illustrates the vertical-root anchoring from Equation (9); curve 2 shows the addition of Equation (10); curve 3 the addition of Equation (8); and curves 4 and 5 add profiles of the frictional strength component with the water table respectively at the surface and 1.0 m below it. The sixth curve represents the downslope component of the colluvium weight, from the left-hand side of Equation (7). Curves 4-6 incorporate the vertically averaged bulk density and the variation of $\tan\phi$ from Equations (11) and (12).

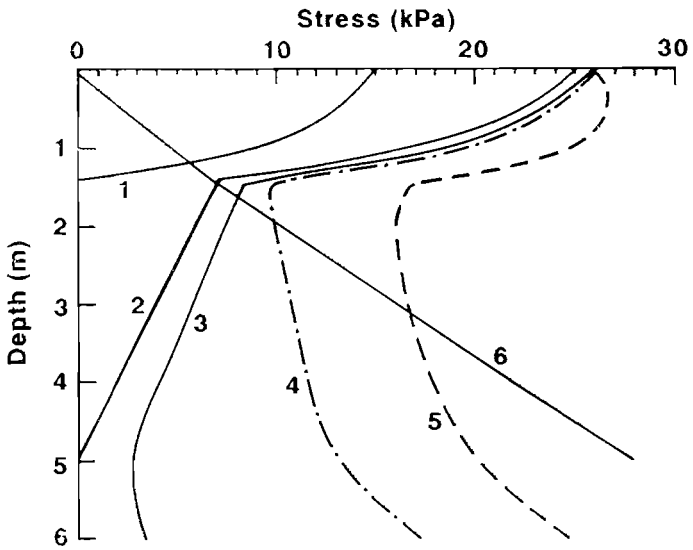

Fig. 9. Schematic profiles of shear resistance components and the downslope component of weight (curve 6) at various depths in colluvium. Curve 1 is the "apparent cohesion" due to vertical anchoring by plant roots; Curve 2 adds to Curve 1 the effects of lateral anchoring and other lateral interactions; Curve 3 continues the addition due to interparticle soil cohesion; Curve 4 adds the frictional component of shear strength for a fully saturated soil, and Curve 5 indicates the frictional strength (added to curve 3) when the water table lies 1 m. below the soil surface.

(3) The saturated thickness of colluvium is calculated by using a simple analytical expression for subsurface flow through a uniform soil in a conical depression. This method, pioneered by Humphrey (1983) and Iida (1984), assumes a pulse of constant-intensity rainfall which recharges the saturated zone without being diminished by storage and transmission in the unsaturated zone. The model also assumes that saturated hydraulic conductivity and unfilled porosity are uniform throughout the colluvium and at the beginning of each storm. These approximations could be relaxed,

but are adequate for the present purpose of illustrating principles.

The peak saturated soil thickness (H, measured normal to the hillslope surface) for any horizontal distance (x) along a cone after a rainstorm of intensity, I (m/hr) and duration, D (hr) is

$$H=Ix(L-0.5x)/K\sin\theta(L-x) \tag{13a}$$

for $x<x_s$, and

$$H=Ix_s(L-0.5x_s)/K\sin\theta(L-x) \tag{13b}$$

for $x>=x_s$. In these equations K (m/hr) is the saturated hydraulic conductivity of the colluvium, θ is the steepness of the cone, and L (m) is its radius. The variable x_s is the distance upslope of which the subsurface discharge has attained steady state by the end of rainfall and is given by

$$x_s=(K\sin\theta\cos\theta D)/p \tag{14}$$

where p is the porosity of the colluvium. The peak value of H is attained long after the end of the storm on the lower parts of the slope, but no pore pressure greater than hydrostatic is allowed in the examples discussed here. Therefore, $H/\cos\theta$ is not allowed to exceed the colluvium depth, z. The value of m in Equation (7) is related to H through $m=h/y$, where

$$h=(H/\cos\theta)-(z-y). \tag{15}$$

(4) The intensity and duration of the rainstorms are selected randomly from independent frequency distributions characterizing the climate. Storms could be selected from the entire distribution of storms, and a frequency distribution of storm arrival times. Since landsliding is usually triggered by large, wet-season storms, the interarrival times and antecedent conditions are ignored in this illustration, although they are obviously important in some events. Annual-maximum series of storms can be randomly generated from probability density functions commonly used for extreme-value analysis in hydrology (e.g., the Gumbel and log-Pierson distributions). However, continuing the strategy of simplicity, I have selected independent intensities and durations of the annual-maximum storms from exponential distributions:

$$\mathrm{f}(I)=\exp(-I/IM) \tag{16}$$

$$\mathrm{f}(D)=\exp(-D/DM) \tag{17}$$

where IM and DM are the means of the annual-maximum intensity and duration.

(5) Each year, the amount of colluvium added to the hollow by weathering, bioturbation and soil creep is distributed uniformly over the cone, thickening the wedge and altering the geotechnical properties at each level. The thickening also increases the

maximum transmissivity of the soil.

Rainstorm intensity and duration are selected from their probability distributions by a random-number generator, and are entered into Equations (13a) and (13b) to predict the peak saturated soil thickness everywhere on the cone. Equation (7) is then examined for critical failure conditions at each depth increment in the soil profile at each distance along the cone. In the examples discussed here, a distance increment of 1.0 m and an elevation increment of 0.1 m were used.

(6) If the annual-maximum storm for the first year does not generate sufficiently high pore pressure to trigger a landslide, a second-year supply of colluvium is spread uniformly over the cone, thickening the soil depth, z. This thickening causes a readjustment of the strength components at each level above the bedrock, as indicated by Fig. 9. When the colluvium is thin, increasing its thickness reduces the minimum strength as the roots are progressively lifted further above the bedrock. If the colluvium is thicker than some critical value, thickening it may slowly increase its strength if cementation and densification slowly increase γ_s and $\tan\phi$. As the soil thickens, its transmissivity also increases, so that the probability of developing a critical value of m in Equation (7) diminishes.

(7) The progressive thickening of colluvium and the random selection of annual-maximum storms eventually trigger a failure at some depth in the colluvium beyond some distance on the cone. It is then assumed that the failure removes all colluvium on the cone below this distance, leaving a landslide scar floored by bedrock. Evacuation is not always complete (e.g., Reneau and Dietrich, 1987), particularly if the lower part of the colluvial profile is old and strong, and this assumption can easily be relaxed since the model calculates the depth at which failure occurs. However, in many steep, bedrock hollows where the residence time of colluvium is less than 10^4 years, complete removal is common. Field measurements (e.g., by Lehre, 1982) illustrate that the margins of landslide scars erode rapidly and some of the sediment thus mobilized leaves the scar by various transport processes. Field observations led Dietrich and Dunne (1978) to propose that emerging seepage would wash all but the coarsest particles out of a bedrock hollow during the early years after failure. However, the accumulations of coarse particles and a fining-upward trend would occur at the base of some colluvial accumulations as the trapping efficiency of the scar increased because of the growth of vegetation and because the thickening of the colluvium would allow more water to be conveyed below the surface.

It would be desirable to model the accelerated diffusion of soil towards the scar, the acceleration of bedrock weathering which occurs in many evacuated hollows, and the trapping efficiency of the healing landslide scar. However, in this initial illustration of principles, trapping is ignored, and the acceleration of weathering and diffusion

are represented crudely by adding each succeeding year's supply of colluvium to the scar, while holding soil depth constant in the rest of the hollow.

The model keeps track of the locations of landslide headscarps and the differences in shear strength and transmissivity which result from the changing depths of colluvium. More than one scar and headscarp can occur at one time. When all scars are filled, the colluvium supply is once again spread uniformly over the cone until the next failure occurs.

(8) The model keeps track of the timing, frequency, extent, depth, and volume of all failures from a bedrock hollow with a chosen geometry and climatic environment. It is typically run for 100,000 years to accumulate statistics on these characteristics of landsliding and the episodic supply of sediment to stream channels by debris flows, analyzed by Benda and Dunne (1987).

Typical results are shown in Figure 10. The simulation involved a conical bedrock hollow with a planimetric radius of 100 m and a planimetric slope length of 90 m. The steepness was 20° and the convergence angle 30°. Colluvium was added to the

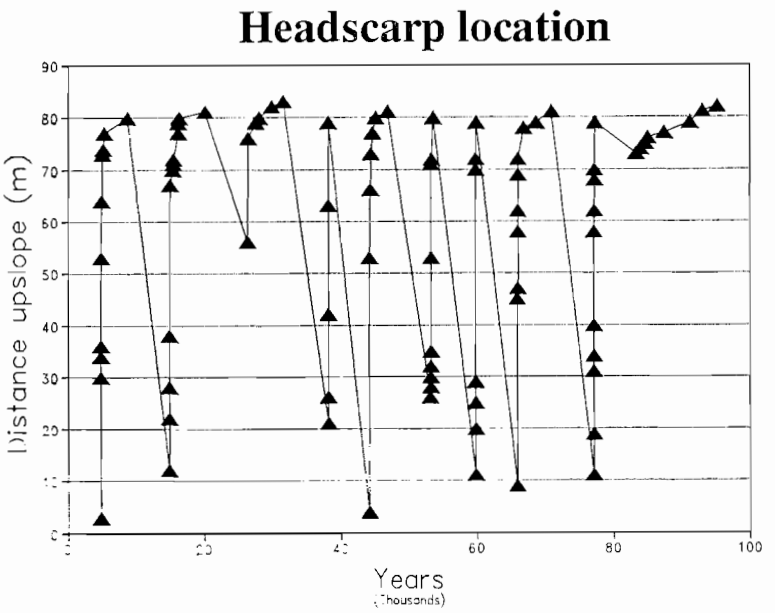

Fig. 10. Sample output from the model of the filling and evacuation of bedrock hollows under a colluvium production rate of 386 $m^3/km^2/yr$. The triangles indicate locations of the headscarp furthest upslope at various times during a 100,000-year period of constant climate represented by independent exponential frequency distributions with a mean annual-maximum rainstorm intensity of 10 mm/hr, and a mean duration of 24 hr. The slope angle was 20° and the convergence angle was 30°.

cone at the rate of 1 m^3/yr, equivalent to a sediment production rate of 386 m^3/km^2/yr. The accumulating colluvium was subjected to a random sequence of storms drawn from independent exponential distributions of annual-maximum storms with a mean intensity of 10 mm/hr and a mean duration of 24 hr. Thus, the simulated conditions were typical of a forested area with rapidly weathering rocks, and large storms. Figure 10 shows the distances upslope at which failures occurred throughout 100,000 simulated years. Landslides occurred in 10 sequences with an average time between sequence initiation of 8700 yrs and a standard deviation of 2500 yrs. Each sequence began with a failure relatively low in the hollow where the probability of full profile saturation was high when the soil depth had increased to 1.95 m. According to curves 4 and 6 in Figure 9, this is the shallowest depth at which the downslope component of weight can exceed the shear resistance of the colluvium if the water table is at the surface. Further upslope or in smaller storms, the colluvium would not fail unless it were deeper than 1.95 m.

After the failure, the model calculates the volume of the scar (which, with the simple conical geometry used here for illustration, is unrealistically wide at the headscarp) and the sediment influx to the stream channel. Rapid diffusion of colluvium into the scar causes the soil depth there to increase while the soil depth above the headscarp is held constant. If the spatial pattern of diffusion were to be modelled explicitly, the colluvium around the headscarp would thin for some interval, diminishing the probability of a landslide there. However, in the current formulation the colluvium upslope remains at constant depth until the scar is filled. The climatic characteristics used in the computation make it unlikely that the colluvium above the first headscarp will survive for long, and in each sequence in Figure 10, failure occurs at successive positions upslope. The interval between failures generally increases as the drainage area above the headscarp decreases, until that interval becomes so large that the scar can be filled to the critical depth for failure with full saturation. At that time a landslide originates low in the hollow again, and the sequence is repeated.

Each landslide scours all colluvium stored downslope of it. Thus, there is a direct relationship between the frequency of scouring and distance downslope. In the case illustrated in Figure 10, 84 landslides occurred in 100,000 years at the base of the slope, whereas only 38 occurred 70 m upslope. There is a zone at the upper end of the cone where failure is exceedingly rare, the colluvium is old, and the soil in its root zone probably diffuses only slowly downslope. For the geometry and geotechnical properties hypothesized here, this stable zone was 7–10 m wide with a mean annual-maximum storm of 10 mm/hr for 24 hr, and 18–25 m wide for a mean storm of 3 mm/hr for 24 hr. It was also 20–25 m wide when the mean rainstorm characteristics were set at 3 mm/hr and 24 hr, and the colluvium supply rate was set at the equivalent of

100 $m^3/km^2/yr$. These latter values are typical of mountains in the Northwestern United States, and for them the model indicates that the lower ends of hollows with a radius of 100 m would be scoured with an average recurrence interval of approximately 3000 yrs, while the recurrence interval between scouring events would rise approximately to 5000 yrs at 50 m upslope and 9000 yrs at 70 m upslope (Figure 11).

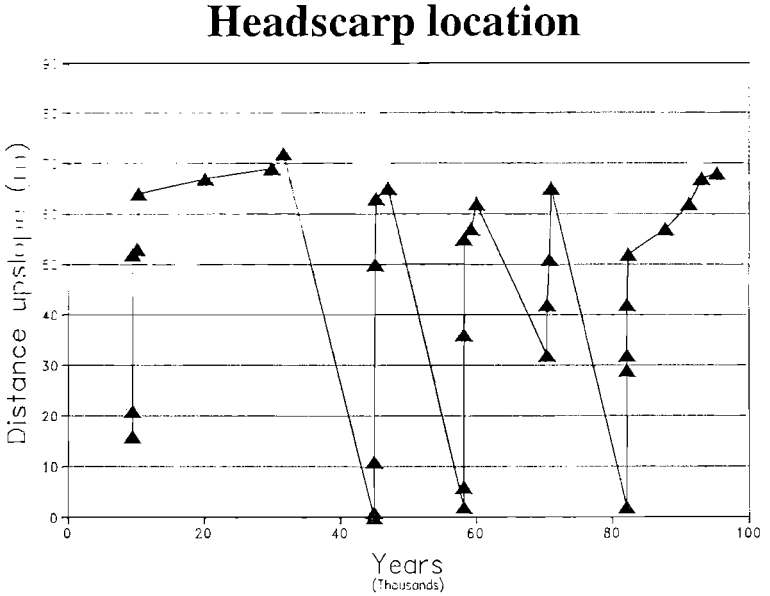

Fig. 11. Sample output from the model for a bedrock hollow with a slope and a convergence angle of 30° under a colluvium production rate of 100 $m^3/km^2/yr$, a mean annual-maximum storm intensity of 3 mm/hr and a mean duration of 24 hours.

The absolute magnitudes of model predictions are probably not accurate, because they depend on the *ad hoc* estimation of model parameters and geometry. In particular, full saturation within a few decameters of the divide in steep bedrock hollows is not widely observed, suggesting that the cone, at least with a convergence angle of 30°, may be an unrealistic approximation to mountain terrain. Its applicability remains to be explored. However, the use of a simple cone approximation and the other arbitrary choices of parameters are meant only to emphasize some general principles. Failure is randomly episodic; it occurs in sequences that cause a headscarp to migrate upslope at a diminishing rate; the lower ends of bedrock hollows are scoured more frequently than the upper zones which fail rarely and under favorable circumstances may accumulate thick, old colluvium which is transported downslope only by slow soil creep of its upper, biogenically disturbed layer. Even if a climatic change were to

alter rainfall and vegetation rooting characteristics, for instance, and expand these relatively stable upper zones, the lower part of the hollow, though being scoured at a decreased rate, would still be subject to relatively frequent landsliding.

The examination of a 100,000-year stationary climate with random variations around its mean is instructive from a theoretical point of view, but records of environmental history indicate that climatic changes should have complicated the colluvial history of bedrock hollows. In principle, this subject may be explored by altering the probability densities for rainstorm intensity and size, and by altering other climatically related parameters in Equation (7). However, the problem is so complex that it is not likely to be solved in detail. Paleoenvironmental records usually yield only mean annual temperature and rainfall, sometimes seasonality, and the regional flora. It is not yet obvious how to retrieve the probabilities of rainstorm characteristics from such data, except possibly by analyzing the relationship between mean annual precipitation and rainstorm probabilities in modern instrumental records from various regions, and then substituting space for time. Changes in root strength could be estimated from records of regional flora, and changes in the frequency of forest fires that affect root strength might be estimated from charcoal buried in colluvium. The effects of weathering and compaction on strength are not yet understood well for current conditions, so it seems premature to estimate the effects of climatic change on these processes. The role of climate in colluvium production by weathering and in biogenic transport also require further study.

Summary

Reconciling the concerns of climatic geomorphology with the type of understanding gained from event-based process geomorphology requires modeling results over the entire spectrum of rainstorm intensity and duration comprising a climate, and also explicitly taking into account those other controls such as vegetation characteristics that vary with climate. This paper describes two small fragments of the larger problem to illustrate how several interesting aspects of geomorphology (and hydrology) reflect the stochastic nature of storms and their interaction with temporal trends in hillslope morphology or in the geotechnical properties of colluvium. There is potential for developing more sophisticated models of these interactions, and an even greater need for focussed field studies to quantify critical processes or relationships that govern the co-evolution of landscape form, colluvial properties, and vegetation.

Acknowledgement

Research described in this paper was supported by National Science Foundation

grant EAR8518058A01.

References Cited

Ahnert, F. (1976) Brief description of a comprehensive three-dimensional process-response model of landform development: Zeitschrift für Geomorphologie, Suppl. Bd, **25**, 29-49.

Band, L. E. (1985) Simulation of slope development and the magnitude and frequency of overland flow erosion in an abandoned hydraulic gold mine: *In* Woldenberg M., ed., *Models in Geomorphology*, Allen & Unwin, London, 191-212.

Benda, L. and Dunne, T. (1987) Sediment routing by debris flow: International Association for Hydrological Sciences Pub. **165**, 213-223.

Beven, K. (1986) Hillslope runoff processes and flood frequency characteristics: *In* Abrahams, A. D. ed., *Hillslope Processes*. Allen & Unwin, London, 187-202.

Burroughs, E. R. Jr. (1984) Landslide hazard rating for portions of the Oregon Coast Range, in: *Proc. Symp on Effects of Forest Land Use on Erosion and Slope Stability*, Environment and Policy Inst., Univ. of Hawaii. Honolulu, 265-274.

Carson, M. A. and Kirkby, M. J. 1972 *Hillslope Form and Process*; Cambridge Univ. Press, Cambridge. 475 p.

Carson, M. A. and Petley, D. J. 1970 The existence of threshold slopes in the denudation of the landscape: Inst. of Brit. Geog. Trans., **49**, 71-95.

DePloey, J. and Savat, 1968 Contribution a l'étude d'érosion par le splash: Zeitschrift für Geomorphologie, **12**. 174-193.

Derbyshire, E. ed., 1973 *Climatic Geomorphology*, Macmillan, London, 296 p.

Derbyshire, E. (ed.) 1976 *Geomorphology and Climate*, Wiley & Sons, London, 512 p.

Dietrich, W. E. and Dunne, T. 1978 Sediment budget for a small catchment in mountainous terrain: Zeitschrift für Geomorphologie, Suppl. Bd., **29**, 191-206.

Dietrich, W. E., Dunne, T., Humphrey, N. F., and Reid, L. M. (1982) Construction of sediment budgets for drainage basins: *In Sediment Budgets and Routing in Forested Drainage Basins*, U. S. Forest Service General Tech. Rept. PNW-141, 5-23.

Dietrich, W. E., Wilson, C. J., and Reneau, S. L. (1986) Hollows, colluvium, and landslides in soil-mantled landscapes: *In* Abrahams, A. D. ed., *Hillslope Processes*, Allen & Unwin, London, 361-388.

Dunne, T. (1978) Field studies of hillslope flow processes: *In* Kirkby, M. J. ed., *Hillslove Hydrology*, Wiley & Sons, Chichester, 227-293.

Dunne, T. and Dietrich, W. E. (1980) Experimental study of Horton overland flow on tropical hillslopes. I: Soil conditions, infiltration, and frequency of runoff. II. Sheetflow hydraulics and hillslope hydrographs: Zeitschrift für Geomorphologie, Suppl. Bd., **33**, 40-80.

Dunne, T., Dietrich, W. E., and Brunengo, M. J. (1980) Simple, portable equipment for erosion experiments under artificial rainstorms: Jour. Agric. Eng. Res., **25**, 1-8.

Hirano, M. (1968) A mathematical model of slope development: an approach to the analytical theory of erosional topography: J. Geosciences Osaka City Univ., **11**, 13-52.

Horton, R. E. 1945. Erosional development of streams and their drainage basins: hydrophysical approach to quantitative morphology: Geol. Soc. Amer. Bull., **56**, 275-370.

Humphrey, N. F. 1983, *Pore pressures in debris failure initiation*: M. S. thesis, Dept. of Geol. Sci., University of Washington; Rept. A-108-WASH, Office of Water Resource Technology (NTIS #PB53 182139).

Iida, T. (1984) A hydrological method of estimation of the topographic effect on the saturated throughflow: Japanese Geomorph. Union Trans., **5**, 1-12.

Kirkby, M. J. (1971) Hillslope process-response models based on the continuity equation: Institute of British Geographers Spec. Pub. **3**, 15-30.

Kirkby, M. J. (1976) Hydrological slope models: the influence of climate: *In* Derbyshire, E. ed., *Geomorphology and Climate*, Wiley & Sons, London, 247–268.

Kirkby, M. J. (1986) A two-dimensional simulation model for slope and stream evolution: *In* Abrahams, A. D., ed., *Hillslope Processes*, Allen & Unwin, London, 203–222.

Lehre, A. K. (1982) Sediment budget of a small Coast Range drainage basin in north-central California: *In Sediment Budgets and Routing in Forested Drainage Basins*, US Forest Service General Technical Report PNW-141, 67–77.

Mosley, M. P. (1973) Rainsplash and the convexity of badland divides: Zeitschrift für Geomorphologie, Suppl. Bd. **18**, 10–25.

Okunishi, K. (1981) Hydrologic analysis in predicting topographic changes: Japanese Geomorph. Union Trans., **2**, 59–65, (Japanese with English abstract).

Okunishi, K. and Iida, T. (1981) Evolution of hillslopes including landslides: Japanese Geomorph. Union Trans., **2**, 291–300.

Reid, L. M. (1989) *Channel incision by surface runoff in grassland catchments*: Ph. D. dissertation, Dept. of Geol. Sci., University of Washington, 199 p.

Reneau, S. L., Dietrich, W. E., Dorn, R. L., Berger, C. R. and Rubin, M. (1986) Geomorphic and paleoclimatic implications of latest Pleistocene radiocarbon dates from colluvium-mantled hollows: Geology, **14**, 655–658.

Reneau, S. L. and Dietrich, W. E. (1987) Size and location of colluvial landslides in a steep forested landscape: Internat. Assoc. Hydrol., Sci. Pub., **165**, 39–48.

Roth, G., Siccardi, S. and Rosso, R. (1989) Hydrodynamic description of the erosional development of drainage patterns: Water Resour. Res., **25**, 319–322.

Shimokawa, E. (1984) A natural recovery process of vegetation on landslide scars and landslide periodicity in forested drainage basin: *In Proc. Symp. on Effect of Forest Land Use on Erosion and Slope Stability*, Environment and Policy Inst., Univ. of Hawaii, Honolulu, 99–107.

Shimokawa, E., Jitousono, T. and Takano, S. (1989) Periodicity of shallow landslide on Shirasu (Ito pyroclastic flow deposits) steep slopes and prediction of potential landslide sites: Japanese Geomorph. Union Trans., **10**, 267–284.

Smith, T. R. and Bretherton, F. P. (1972) Stability and conservation of mass in drainage basin evolution: Water Resour. Res., **8**, 1506–1529.

Tsukamoto, Y., Ohta, T. and Noguchi, H. (1982) Hydrological and geomorphological studies of debris slides on forested hillslopes in Japan: Internal Assoc. Hydrol. Sci. Pub. **137**, 89–98.

Tsukamoto, Y. and Kusakabe, O. (1984) Vegetative influences on debris slide occurrences on steep slopes in Japan: *In Proc. Symp. on Effect of Forest Land Use on Erosion and Slope Stability*, Environment and Policy Inst., Univ. of Hawaii, Honolulu, 63–72.

Tsukamoto, Y. and Minematsu, H. (1986) Evaluation of the effect of lateral roots on slope stability: Internat. Union For. Res. Org. Congress, Ljubliana.

Wilson, C. J. and Dietrich, W. E. (1987) The contribution of bedrock groundwater flow to storm runoff and pore pressure development in hollows: Internat. Assoc. of Hydrol. Sci. Pub. **165**, 49–59.